Biochemical and Biophysical Research Communications 428 (2012) 321–326

Contents lists available at SciVerse ScienceDirect

Biochemical and Biophysical Research Communications

journal homepage: www.elsevier.com/locate/ybbrc

Carbachol ameliorates lipopolysaccharide-induced intestinal epithelial tight junction damage by down-regulating NF-κβ and myosin light-chain kinase pathways

Ying Zhang, Jianguo Li *

Department of Anesthesia, Critical Care Medicine & Emergency Medicine Center, Zhongnan Hospital, Wuhan University, Wuhan 430071, Hubei Province, People's Republic of China

ARTICLE INFO

Article history:
Received 25 September 2012
Available online 23 October 2012

Keywords:
Carbachol
Nuclear factor-kappa beta
Myosin light-chain kinase
Tight junction
Intestinal permeability

ABSTRACT

Carbachol is a cholinergic agonist that protects the intestines after trauma or burn injury. The present study determines the beneficial effects of carbachol and the mechanisms by which it ameliorates the lipopolysaccharide (LPS)-induced intestinal barrier breakdown. Rats were injected intraperitoneally with 10 mg/kg LPS. Results showed that the gut barrier permeability was reduced, the ultrastructural disruption of tight junctions (TJs) was prevented, the redistribution of zonula occludens-1 and claudin-2 proteins was partially reversed, and the nuclear factor-kappa beta (NF-κβ) and myosin light-chain kinase (MLCK) activation in the intestinal epithelium were suppressed after carbachol administration in LPS-exposed rats. Pretreatment with the α7 nicotinic acetylcholine receptor (α7nAchR) antagonist α-bungarotoxin blocked the protective action of carbachol. These results suggested that carbachol treatment can protect LPS-induced intestinal barrier dysfunction. Carbachol exerts its beneficial effect on the amelioration of the TJ damage by inhibiting the NF-κβ and MLCK pathways in an α7nAchR-dependent manner.

1. Introduction

Sepsis is one of the primary causes of patient death in the intensive care units, and mainly occurs in response to lipopolysaccharide (LPS). Over the past three decades, new strategies for sepsis treatment have been developed. However, its morbidity and mortality in critically ill patients remain significantly high [1]. The exact mechanisms behind sepsis development remain unclear. Meanwhile, gut dysfunction has been identified in sepsis, and increased intestinal permeability has been found associated with the development of multiple organ dysfunction [2,3]. Thus, an intact and functional mucosal barrier, maintained by the intestinal epithelium, is crucial in preventing the translocation of enteric bacteria and microbial pathogens, both paracellularly and transcellularly [4]. Therefore, the protection of the gut barrier function is critical during sepsis treatment.

The tight junctions (TJs), such as the zonula occludens (ZO)-1 [5] and the claudin family members [6], are critical in the paracellular characteization of the intestinal barrier. Previous studies have indicated that the TJ architecture and the protein redistribution in the TJ membrane microdomains are altered during polymicrobial sepsis [7]. In addition, the TJ opening is driven by myosin light-chain (MLC) phosphorylation, which is dependent on MLC kinase (MLCK) activation [8]. Moriez et al. [9] have reported that the inhibition of MLCK prevents the harmful effects of the LPS-induced sepsis on the TJ barrier. Moreover, the nuclear factor-kappa beta (NF-κβ) signaling pathway mediates the increased MLCK expression after LPS induction, resulting in TJ barrier breakdown [10]. Therefore, the inhibitors of NF-κβ and MLCK functions may attenuate TJ disruption [11,12].

Carbachol has been widely applied clinical applications because of its muscarinic effect, which promotes intestinal peristalsis and increases glandular secretion. Recent studies have found various pharmacologic and biologic activities associated with carbachol, including anti-inflammatory [13], antioxidative [14], and anti-apoptotic [15] effects. In vivo studies have indicated that the anti-inflammatory activities displayed by carbachol may be partly mediated by suppressing the NF-κβ activation pathway [16]. Carbachol can also attenuate intestinal dysfunction after trauma or burn injury [17]. However, the protective potential of carbachol for intestinal barrier function in endotoxemia has not been reported. Therefore, we hypothesize that carbachol ameliorates the LPS-induced intestinal epithelial TJ damage.

2. Materials and methods

2.1. Experimental animals

Male Sprague–Dawley rats (Wuhan Universtity Experiment Animals Center) weighing 200–250 g were used for the experiment. All animals were maintained in a sterile, standard laboratory

* Corresponding author. Fax: +86 027 67813190.
E-mail address: 2010lijianguo@sina.cn (J. Li).

0006-291X/$ - see front matter © 2012 Elsevier Inc. All rights reserved.
http://dx.doi.org/10.1016/j.bbrc.2012.10.056

supplied with food and water as needed. The rats were placed in individual ventilated cages under specific pathogen-free conditions in the animal facility of Wuhan University. All protocols were approved by the Wuhan University of Science and Technology Animal Care and Use Committee. In addition, the animals received humane care in compliance with the Principles of Laboratory Animal Care.

2.2. Reagents

The LPS from the *Escherichia coli* serotype 055:B7, α-bungarotoxin (α-BGT), 4 KDa fluorescein isothiocyanate-dextran (FITC-Dextran), carbachol, and MLCK antibody were purchased from Sigma Chemical Co. (St.Louis, MO, USA). The antibodies for ZO-1, claudin-2, and NF-κβ p65 were purchased from Invitrogen. The FITC-conjugated affinipure goat anti-rabbit immunoglobulin G (IgG) were purchased from Molecular Probes.

2.3. Experiment protocols

The rats were divided randomly into four groups, namely, control (CON group), LPS, carbachol (CAR group), and α-BGT groups, with eight rats in each group. In the LPS group, rats were injected intraperitoneally with 10 mg/kg LPS dissolved in 1 ml sterile saline. In the CON group, rats were treated in the same manner as that of the LPS group, but they received saline instead of LPS. In the CAR group, rats were injected intraperitoneally with 0.1 mg/kg carbachol at 15 min after LPS injection. In the α-BGT group, rats were first exposed to LPS, and then injected with 1.0 μg/kg α-BGT at 5 min prior to carbachol injection. The samples were collected after 3 h of LPS treatment.

2.4. Histopathological evaluation

The distal ileum (5 cm) was harvested immediately after the rats were sacrificed, and then the specimens were embedded in paraffin. The ileac tissues were deparaffinized, rehydrated, and stained with hematoxylin and eosin (H&E). Histologic scoring of the depth of tissue injury was performed according to the method by Chiu et al. [18], with modifications on the score as follows: 0, no damage; 1, subepithelial space at the villous tip; 2, loss of mucosal lining of the villous tip; 3, loss of less than half of the villous structure; 4, loss of more than half of the villous structure; and 5, transmural necrosis. The tissues were evaluated blindly without prior knowledge of the animal background.

2.5. Quantification of intestinal permeability

Three hours after LPS induction, 5 cm of the terminal ileum and the right side colon were removed. The intestinal lumen was gently washed, and one side of the intestine was ligated. A 200 μl of 40 mg/ml 4-KDa FITC-Dextran was applied onto the intestinal lumen, and then its other side was ligated. The intestinal pouch was immersed gently in 10 ml of saline at 37 °C for 60 min. The intestinal wall permeability was evaluated ex vivo by measuring the leaked amount of FITC-dextran outside the intestinal pouch.

2.6. Transmission electron microscopy of TJ

The 2-mm sections of the ileum were washed and fixed with 4% glutaraldehyde for 2 h, post-fixed with 1% osmium tetroxide, embedded in Epon 812, and then thinly sliced. The thinly sliced tissues were cut, stained with uranyl acetate and lead citrate, and then examined in an H-600 (Hitachi, Japan) transmission electron microscope (TEM) operated at 75 kV.

2.7. Immunofluorescence microscopy

The small intestine tissue samples in rats were frozen using liquid nitrogen, and then the frozen sections (15 μm) were cut within a cryostat. The resulting tissue samples were incubated with the first antibodies anti-ZO-1 and anti-claudin-2 overnight at 4 °C, and then with FITC-conjugated goat anti-rabbit IgG antibodies. The sample images were obtained using an LSM 410 confocal laser scanning microscope (Leica Microsystems; Heidelberg).

2.8. Immunohistochemistry microscopy

The tissues were stained with H&E, and then incubated with anti-MLCK for 24 h at 4 °C, secondary antibody-biotinylated anti-rabbit IgG for 30 min, and peroxidase-conjugated streptavidin for 30 min. Phosphate buffer saline was used to rinse the slides following each incubation. The color was developed using 0.025% 3,3′-diaminobenzidine tetrahydrochloride in tris buffered saline combined with hydrogen peroxide. The specimens were counterstained, dehydrated, mounted, observed by light microscopy (ECLIPSE E600; Nikon, Tokyo, Japan), and then photographed (DXM1200; Nikon).

2.9. Tissue nuclear protein extraction

The nuclear extracts were prepared following a previous protocol [19]. The homogenates were centrifuged at 14,000 rpm for 5 min, and the supernatant nuclear extracts were then harvested and stored at −70 °C. The extracted proteins were quantified by Lowry–Kalckar assays [20].

2.10. Western blot analysis

Western blot analysis was carried out to measure the protein expressions of ZO-1, claudin-2, NF-κβ, and MLCK. Equal amounts of each extract were electrophoresed in 6% sodium dodecyl sulfate–polyacrylamide gel electrophoresis, electrotransferred onto polyvinylidene difluoride membranes (Bio-Rad), and then incubated with the primary antibody overnight at 4 °C and with the secondary antibodies for 90 min at room temperature. The bands were detected by enhanced chemiluminescence, and the band intensities were quantified by densitometry and expressed as mean area density using the accompanied software. Mean area density was expressed for all protein blots relative to glyceraldehyde-phosphate dehydrogenase(GAPDH) expression.

2.11. Statistical analysis

Data were presented as mean ± SEM, and compared through one-way analysis of variance(ANOVA). The Student-Newman-Keuls q test was used for statistical analysis to compare the data among all groups. A significant difference was presumed when $P < 0.05$.

3. Results

3.1. Effect of carbachol on LPS-induced intestinal barrier breakdown

The histologic changes and injury score after carbachol treatment in LPS-exposed rats were determined to evaluate the effects of carbachol on intestinal injury. The histological examination for the LPS group revealed significantly damaged intestinal tissues, with villus necrosis, inflammatory cell infiltration, and hemorrhage. However, these histologic changes were less pronounced in the CAR group. The appearance of the α-BGT group resembled that of the LPS group (Fig. 1A). The intestinal histological score for the LPS group was significantly increased compared with the

CON group ($^{\triangle}P < 0.05$). Carbachol treatment remarkably decreased the mucosal damage in the LPS group ($^{*}P < 0.05$). α-BGT administration reversed the effect of carbachol ($^{\#}P < 0.05$, Fig. 1B).

Three hours after LPS induction, we evaluated the gut mucosal permeability ex vivo by measuring the leakage of FITC-Dextran from the intestinal pouch. The amount of FITC-Dextran significantly increased after LPS administration ($^{\triangle}P < 0.05$). However, this increased amount was significantly reduced after carbachol administration ($^{*}P < 0.05$). Increased amounts of FITC-Dextran were observed after α-BGT pretreatment compared with the CAR group ($^{\#}P < 0.05$, Fig. 1C).

3.2. Effect of carbachol on the LPS-induced intestinal TJ disruption

The ultrastructure of TJ in the ileum was observed by TEM to determine the influence of carbachol on the LPS-induced intestinal TJ disruption. The TJs were damaged and the electron-dense materials were diminished in the LPS group. The pathologic changes induced by LPS were significantly attenuated by carbachol, whereas α-BGT pretreatment diminished the beneficial effect of carbachol (Fig. 2A).

Three hours after LPS administration, the localization and expression of ZO-1 and claudin-2 proteins were determined by immunofluorescence and Western blotting. ZO-1 and claudin-2 staining at the areas of cell–cell contact were significantly lost in the LPS group. These local losses were improved by carbachol treatment, with continuous staining observed at the periphery of the intestinal epithelial cells. The ZO-1 and claudin-2 expressions were highly attenuated in the α-BGT group than those in the CAR group (Fig. 2B). Fig. 2C shows that the ZO-1 and claudin-2 protein expressions from the intestinal tissues of the LPS and CON groups were significantly different ($^{\triangle}P < 0.05$). Carbachol treatment significantly increased the ZO-1 and claudin-2 protein expressions in the lieum of the LPS group ($^{*}P < 0.05$), whereas α-BGT diminished the effect of carbachol ($^{\#}P < 0.05$).

3.3. Effect of carbachol on the NF-κβ and MLCK pathways in the intestinal tissues of LPS-treated rats

We examined the effect of carbachol on NF-κβ and MLCK activation to investigate the mechanisms behind the attenuation of intestinal epithelial TJ damage by carbachol. Fig. 3A shows that

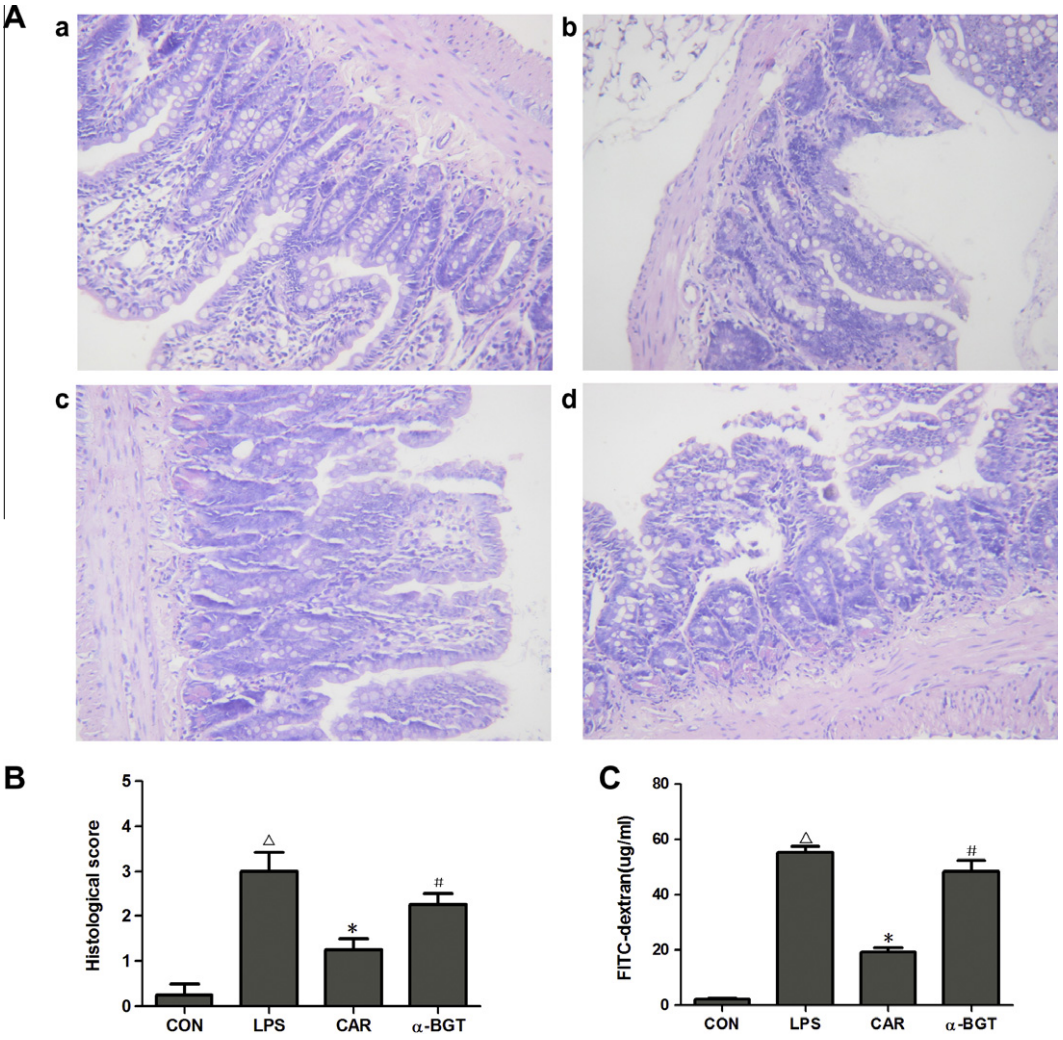

Fig. 1. Effect of carbachol on LPS-induced intestinal barrier breakdown. Carbachol was injected intraperitoneally at 15 min after LPS injection. (A) Effects of carbachol on LPS-mediated ileum histopathologic changes. Ilea ($n = 3$) from each experimental group were processed for histological evaluation at 3 h after LPS induction: ileum section of the (a) CON group; (b) LPS group; (c) CAR group; and (d) α-BGT group. The representative histologic sections of the ilea were stained by H&E at 200× magnification. (B) Effects of carbachol on intestinal injury score. The intestinal injury score was determined at 3 h after LPS administration. The values were presented as means ± SEM ($n = 8$). $^{\triangle}P < 0.05$ vs. CON group. $^{*}P < 0.05$ vs. LPS group. $^{\#}P < 0.05$ vs. CAR group. (C) Effects of carbachol on LPS-induced increased ileal mucosal permeability. The leakage of FITC-Dextran from the intestinal pouch was measured at 3 h after LPS administration. The values were presented as means ± SEM ($n = 8$). $^{\triangle}P < 0.05$ vs. CON group. $^{*}P < 0.05$ vs. LPS group. $^{\#}P < 0.05$ vs. CAR group.

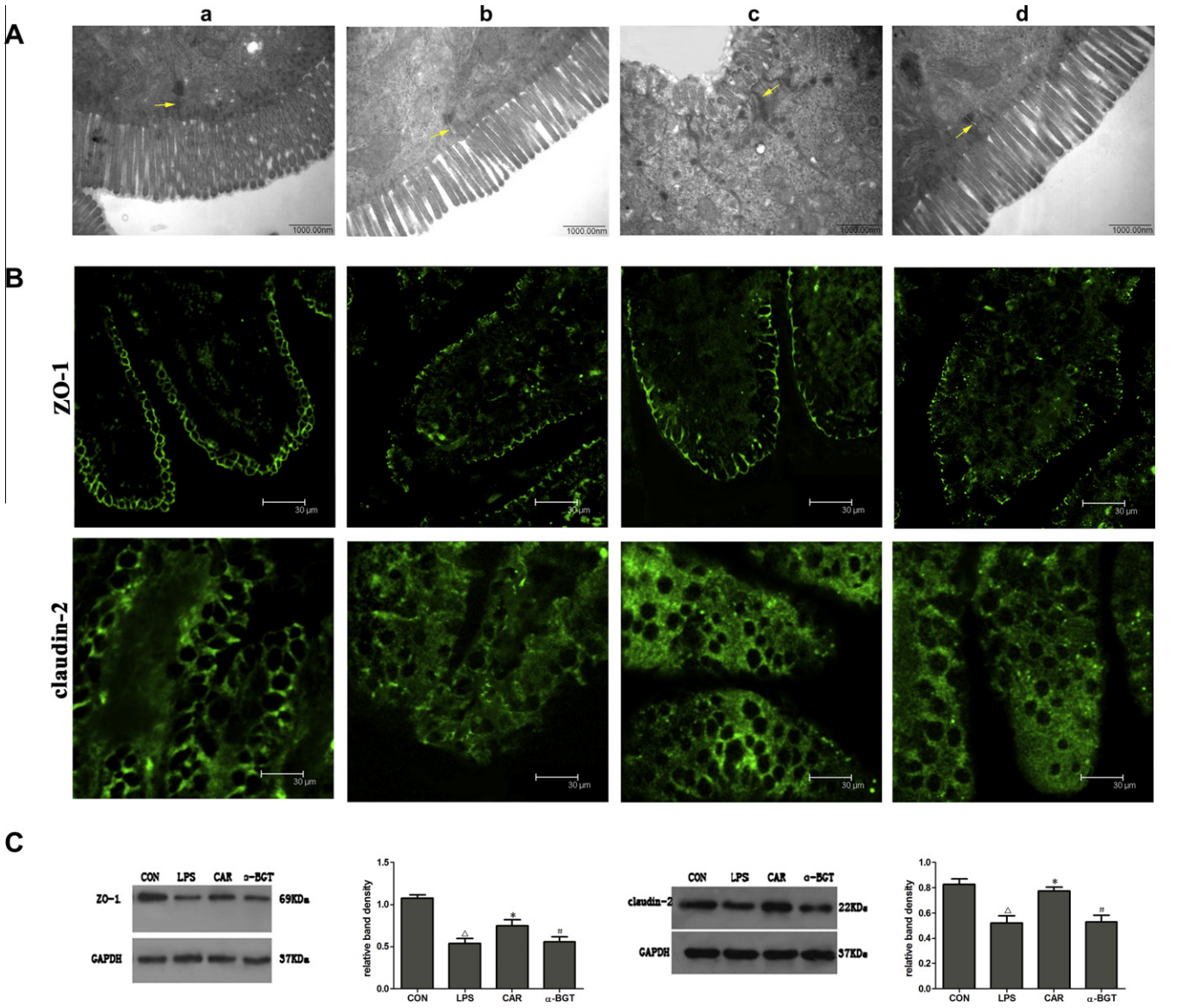

Fig. 2. Effect of carbachol on LPS-induced intestinal TJ disruption. Carbachol was injected intraperitoneally at 15 min after LPS administration. Ilea ($n = 3$) from each experimental group were processed for morphological evaluation at 3 h after LPS administration:ileum section from the (a) CON group; (b) LPS group; (c) CAR group; (d) α-BGT group. (A) Effect of carbachol on intestinal TJ ultrastructure after LPS induction. Arrows indicate the location of the TJs (Scale bar = 1000 nm). (B) Effect of carbachol on the localization of intestinal TJ proteins, ZO-1 and claudin-2, at 3 h after LPS exposure (scale bar = 30μm). (C) Effect of carbachol on the expression of intestinal TJ proteins ZO-1 and claudin-2 3 h after LPS induction. Protein samples were analyzed by Western blotting, and GAPDH was used as an internal control. Similar results were obtained among three independent experiments. The result of one of the experiments is shown. $^{\triangle}P < 0.05$ vs. CON group. $^{*}P < 0.05$ vs. LPS group. $^{\#}P < 0.05$ vs. CAR group.

the nuclear expressions of NF-κβ and MLCK increased in the LPS group ($^{\triangle}P < 0.05$). Carbachol significantly attenuated the NF-κβ and MLCK expressions ($^{*}P < 0.05$). α-BGT administration reversed the inhibitory effect of carbachol ($^{\#}P < 0.05$).

Three hours after LPS administration, we evaluated the MLCK activation using immunohistochemistry. MLCK was expressed at the periphery of the intestinal epithelial cells, as reflected by the brown staining images under the light microscope. Increased MLCK staining was observed in the LPS group compared with the CON group. Carbachol treatment decreased MLCK staining, whereas α-BGT administration diminished the inhibitory effect of carbachol (Fig. 3B).

4. Discussion

To the best of our knowledge, the current study was the first to demonstrate that carbachol protects rats against LPS-induced intestinal barrier breakdown. The protective effects of carbachol were associated with the down-regulation of the NF-κβ and MLCK pathways.

The intestinal epithelial barrier is important in the systemic inflammatory response after LPS induction. Its breakdown is characterized by high gut permeability, decreased mucosal weight, and typical histologic changes, such as villus necrosis, inflammatory cell infiltration, and decreased villus height [21]. In the present study, carbachol treatment decreased the ileal mucosal permeability to FITC-Dextran, and significantly attenuated intestinal tissue injury.

The intestinal TJ proteins ZO-1 [5] and claudin-2 [6] are key regulators of intestinal permeability; thus, they characterize the intestinal barrier. In vitro studies demonstrated that LPS decreases ZO-1 expression in nontumorgenic epithelial monolayers [22], significantly disrupting barrier function. Several studies have shown that decreased ZO-1 protein expression is correlated with increased

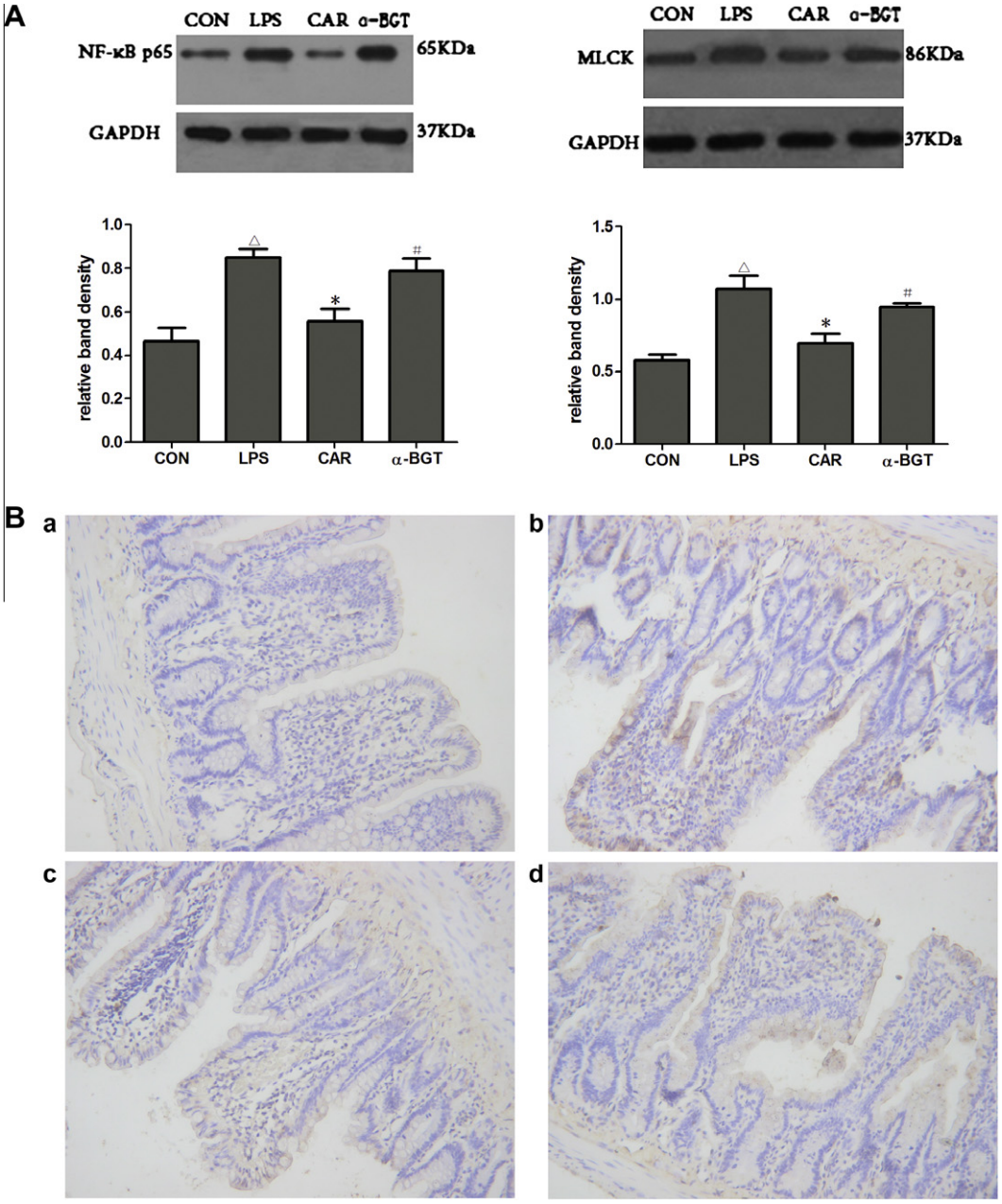

Fig. 3. Effect of carbachol on NF-κβ and MLCK activation in ilea 3 h after LPS induction. Carbachol was injected intraperitoneally at 15 min after LPS injection. (A) Effect of carbachol on NF-κβ and MLCK expressions in ilea at 3 h after LPS induction. Protein samples were analyzed by Western blotting, and GAPDH was used as an internal control. Similar results were obtained among three independent experiments. The result of one of the experiments is shown. $^{\triangle}P < 0.05$ vs. CON group. $^{*}P < 0.05$ vs. LPS group. $^{\#}P < 0.05$ vs. CAR group. (B) Immunohistochemical staining of intestinal sections for MLCK. Ilea ($n = 3$) from each experimental group were processed for histologic evaluation at 3 h after LPS induction: the ileum section from the (a) CON group; (b) LPS group; (c) CAR group; (d) α-BGT group. The brown staining images indicate the location of MLCK at 200× magnification. (For interpretation of the references to colour in this figure legend, the reader is referred to the web version of this article)

paracellular permeability in endotoxemic [11] and thermal [23] animals. The modulation of intestinal claudin-2 expression has been implicated as the cause of inflammatory bowel diseases [24] and collagenous collitis [25]. The results of our study demonstrated that LPS induction caused varying degrees of displacement and down-regulated the expressions of ZO-1 and claudin-2 proteins, thereby resulting in increased intestinal permeability. However, carbachol treatment partially reversed the redistribution and increased permeability of these TJ proteins. Thus, carbachol may effectively prevent the endotoxin-induced TJ disruption.

The NF-κβ and MLCK signaling pathways were investigated after LPS induction to explore the mechanisms behind the beneficial effects of carbachol. MLCK is vital in the regulation of the intestinal barrier function because it modulates the actin–myosin ring. The MLCK-mediated MLC phosphorylation contracted the actin–myosin filaments, thereby altering TJ protein localization and expression as well as TJ barrier functional opening [26]. MLCK activation increases permeability and modulates other important TJs, such as occludin and ZO-1 [27]. The NF-κβ signaling cascade is a common pathway involved in the inflammatory response to diverse stimuli. During endotoxemia, the inhibitory factor κβ in intestinal mucosa is degraded, resulting in cytoplasmic-to-nuclear translocation of NF-κβ p65 [28]. Thereafter, the activated NF-κβ p65 binds to the MLCK promoter region and increases MLCK mRNA expression [29,30]. The results of our study demonstrated that carbachol treatment significantly diminished the activation of NF-κβ

in the intestinal tissue, resulting in the changes in MLCK activation. These results implied that the beneficial effect of carbachol on TJ may be partially mediated by the down-regulating the NF-κβ and MLCK pathways.

Studies have shown that α7 nicotinic acetylcholine receptor (α7nAchR) is an essential inflammatory regulator [31]. Previous studies have reported that α-BGT is a specific antagonist of α7nAchR, which inhibits the effect of acetylcholine in the cholinergic anti-inflammatory pathway by binding α7nAchR. In the present study, the pretreatment with α-BGT blocked the beneficial effect of carbachol on intestinal TJ. This result implied that the protective effect of carbachol on intestinal barrier function depends on the α7nAchR subunit.

In summary, we have provided the first evidence that carbachol treatment protects the LPS-induced intestinal barrier dysfunction by ameliorating TJ damage. The mechanisms behind the beneficial effects of carbachol are correlated with the inhibition of the NF-κβ and MLCK signaling pathways in an α7nAchR-dependent manner. These findings may provide a new therapeutic strategy for the treatment of intestinal barrier breakdown in sepsis.

Acknowledgments

This work was financially supported by the National Natural Science Foundation of China (No. 303162519) and the Key Project of the National Natural Science Foundation of China (No. 30671586).

We are very thankful to Boqun Pan for his excellent technical assistance during the immunofluorescence studies.

References

[1] S. Shinozaki, Y. Inoue, W. Yang, M. Fukaya, E.A. Carter, Y.M. Yu, A. Fischman, R. Tompkins, M. Kaneki, Farnesyltransferase inhibitor improved survival following endotoxin challenge in mice, Biochem. Biophys. Res. Commun. 391 (2010) 1459–1464.

[2] D.A. De-Souza, L.J. Greene, Intestinal permeability and systemic infections in critically ill patients: effect of glutamine, Crit. Care Med. 33 (2005) 1125–1135.

[3] C.J. Doig, L.R. Sutherland, J.D. Sandham, G.H. Fick, M. Verhoef, J.B. Meddings, Increased intestinal permeability is associated with the development of multiple organ dysfunction syndrome in critically ill ICU patients, Am. J. Respir. Crit. Care Med. 158 (1998) 444–451.

[4] J.L. Madara, Warner-Lambert/Parke-Davis Award lecture. Pathobiology of the intestinal epithelial barrier, Am. J. Pathol. 137 (1990) 1273–1281.

[5] B.R. Stevenson, J.D. Siliciano, M.S. Mooseker, D.A. Goodenough, Identification of ZO-1: a high molecular weight polypeptide associated with the tight junction (zonula occludens) in a variety of epithelia, J. Cell Biol. 103 (1986) 755–766.

[6] M. Furuse, H. Sasaki, S. Tsukita, Manner of interaction of heterogeneous claudin species within and between tight junction strands, J. Cell Biol. 147 (1999) 891–903.

[7] Q. Li, Q. Zhang, C. Wang, X. Liu, N. Li, J. Li, Disruption of tight junctions during polymicrobial sepsis in vivo, J. Pathol. 218 (2009) 210–221.

[8] J.R. Turner, Molecular basis of epithelial barrier regulation: from basic mechanisms to clinical application, Am. J. Pathol. 169 (2006) 1901–1909.

[9] R. Moriez, C. Salvador-Cartier, V. Theodorou, J. Fioramonti, H. Eutamene, L. Bueno, Myosin light chain kinase is involved in lipopolysaccharide-induced disruption of colonic epithelial barrier and bacterial translocation in rats, Am. J. Pathol. 167 (2005) 1071–1079.

[10] D. Ye, I. Ma, T.Y. Ma, Molecular mechanism of tumor necrosis factor-alpha modulation of intestinal epithelial tight junction barrier, Am. J. Physiol. Gastrointest. Liver Physiol. 290 (2006) G496–504.

[11] L. Gu, N. Li, J. Gong, Q. Li, W. Zhu, J. Li, Berberine ameliorates intestinal epithelial tight-junction damage and down-regulates myosin light chain kinase pathways in a mouse model of endotoxinemia, J. Infect. Dis. 203 (2011) 1602–1612.

[12] T.W. Costantini, W.H. Loomis, J.G. Putnam, L. Kroll, B.P. Eliceiri, A. Baird, V. Bansal, R. Coimbra, Pentoxifylline modulates intestinal tight junction signaling after burn injury: effects on myosin light chain kinase, J. Trauma 66 (2009) 17–24 (discussion 24-15).

[13] S. Hu, X.G. Jiang, D.G. Shi, Y. Lu, J.Y. Li, D. Sun, Z.Y. Sheng, Carbachol alleviates inflammation in gut tissue during ischemia/reperfusion in rats, Zhongguo Wei Zhong Bing Ji Jiu Yi Xue 15 (2003) 748–750.

[14] S. Hu, L.J. Zhang, H.Y. Bai, C.M. Bao, The protective effects of carbachol on visceral ischemia-induced lipid peroxidation injury in rats with sepsis, Zhongguo Wei Zhong Bing Ji Jiu Yi Xue 21 (2009) 552–554.

[15] S. Hu, X.F. Zou, Y. Lu, J.Y. Lu, Z.Y. Sheng, Effects of carbachol on apoptosis of intestinal epithelial cells after gut ischemia/reperfusion in rat, Zhongguo Wei Zhong Bing Ji Jiu Yi Xue 19 (2007) 463–466.

[16] G. Zhou, S. Hu, Y. Lv, Q. Song, X. Zou, Z. Sheng, Carbachol alleviates rat cytokine release and organ dysfunction induced by lipopolysaccharide, J. Trauma 71 (2011) 157–162.

[17] W.H. Cao, J.K. Chai, S. Hu, H.M. Yang, T.J. Sun, X.F. Zou, Z.Y. Sheng, Influence of carbachol on intestinal dysfunction after traumatic or burn injury, Zhonghua Shao Shang Za Zhi 22 (2006) 168–171.

[18] C.J. Chiu, A.H. McArdle, R. Brown, H.J. Scott, F.N. Gurd, Intestinal mucosal lesion in low-flow states. I. A morphological, hemodynamic, and metabolic reappraisal, Arch. Surg. 101 (1970) 478–483.

[19] X.M. Song, J.G. Li, Y.L. Wang, Z.F. Hu, Q. Zhou, Z.H. Du, B.H. Jia, The protective effect of the cholinergic anti-inflammatory pathway against septic shock in rats, Shock 30 (2008) 468–472.

[20] N.C. Andrews, D.V. Faller, A rapid micropreparation technique for extraction of DNA-binding proteins from limiting numbers of mammalian cells, Nucleic Acids Res. 19 (1991) 2499.

[21] H.M. Li, Y.Y. Wang, H.D. Wang, W.J. Cao, X.H. Yu, D.X. Lu, R.B. Qi, C.F. Hu, Y.X. Yan, Berberine protects against lipopolysaccharide-induced intestinal injury in mice via alpha 2 adrenoceptor-independent mechanisms, Acta Pharmacol. Sin. 32 (2011) 1364–1372.

[22] A.C. Chin, A.N. Flynn, J.P. Fedwick, A.G. Buret, The role of caspase-3 in lipopolysaccharide-mediated disruption of intestinal epithelial tight junctions, Can. J. Physiol. Pharmacol. 84 (2006) 1043–1050.

[23] M. Krzyzaniak, C. Peterson, W. Loomis, A.M. Hageny, P. Wolf, L. Reys, J. Putnam, B. Eliceiri, A. Baird, V. Bansal, R. Coimbra, Postinjury vagal nerve stimulation protects against intestinal epithelial barrier breakdown, J. Trauma 70 (2011) 1168–1175 (discussion 1175-1166).

[24] S. Zeissig, N. Burgel, D. Gunzel, J. Richter, J. Mankertz, U. Wahnschaffe, A.J. Kroesen, M. Zeitz, M. Fromm, J.D. Schulzke, Changes in expression and distribution of claudin 2, 5 and 8 lead to discontinuous tight junctions and barrier dysfunction in active Crohn's disease, Gut 56 (2007) 61–72.

[25] N. Burgel, C. Bojarski, J. Mankertz, M. Zeitz, M. Fromm, J.D. Schulzke, Mechanisms of diarrhea in collagenous colitis, Gastroenterology 123 (2002) 433–443.

[26] H. Ralay Ranaivo, N. Carusio, R. Wangensteen, P. Ohlmann, C. Loichot, A. Tesse, K. Chalupsky, I. Lobysheva, J. Haiech, D.M. Watterson, R. Andriantsitohaina, Protection against endotoxic shock as a consequence of reduced nitrosative stress in MLCK210-null mice, Am. J. Pathol. 170 (2007) 439–446.

[27] L. Shen, E.D. Black, E.D. Witkowski, W.I. Lencer, V. Guerriero, E.E. Schneeberger, J.R. Turner, Myosin light chain phosphorylation regulates barrier function by remodeling tight junction structure, J. Cell Sci. 119 (2006) 2095–2106.

[28] T.A. Pritts, R. Moon, J.E. Fischer, A.L. Salzman, P.O. Hasselgren, Nuclear factor-kappaB is activated in intestinal mucosa during endotoxemia, Arch. Surg. 133 (1998) 1311–1315.

[29] T.Y. Ma, M.A. Boivin, D. Ye, A. Pedram, H.M. Said, Mechanism of TNF-{alpha} modulation of Caco-2 intestinal epithelial tight junction barrier: role of myosin light-chain kinase protein expression, Am. J. Physiol. Gastrointest. Liver Physiol. 288 (2005) G422–G430.

[30] R. Al-Sadi, D. Ye, K. Dokladny, T.Y. Ma, Mechanism of IL-1beta-induced increase in intestinal epithelial tight junction permeability, J. Immunol. 180 (2008) 5653–5661.

[31] H. Wang, M. Yu, M. Ochani, C.A. Amella, M. Tanovic, S. Susarla, J.H. Li, H. Yang, L. Ulloa, Y. Al-Abed, C.J. Czura, K.J. Tracey, Nicotinic acetylcholine receptor alpha7 subunit is an essential regulator of inflammation, Nature 421 (2003) 384–388.